MedChemComm

RESEARCH ARTICLE

View Article Online
View Journal | View Issue

Cite this: *Med. Chem. Commun.*, 2018, **9**, 1920

Structure activity relationship of 2-arylalkynyl-adenine derivatives as human A_3 adenosine receptor antagonists†

Jinha Yu,[a] Philip Mannes,[a] Young-Hwan Jung,[a] Antonella Ciancetta,[b] Amelia Bitant,[c] David I. Lieberman,[a] Sami Khaznadar,[a] John A. Auchampach,[c] Zhan-Guo Gao[a] and Kenneth A. Jacobson *[a]

Received 26th June 2018,
Accepted 23rd September 2018

DOI: 10.1039/c8md00317c

rsc.li/medchemcomm

Recognition of nucleosides at adenosine receptors (ARs) is supported by multiple X-ray structures, but the structure of an adenine complex is unknown. We examined the selectivity of predicted A_1AR and A_3AR adenine antagonists that incorporated known agonist affinity-enhancing N^6 and C2 substituents. Adenines with A_1AR-favoring N^6-alkyl, cycloalkyl and arylalkyl substitutions combined with an A_3AR-favoring 2-((5-chlorothiophen-2-yl)ethynyl) group were human (h) A_3AR-selective, *e.g.* MRS7497 **17** (~1000-fold over A_1AR). In addition, binding selectivity over hA_{2A}AR and hA_{2B}AR and functional A_3AR antagonism were demonstrated. **17** was subjected to computational docking and molecular dynamics simulation in a hA_3AR homology model to predict interactions. The SAR of nucleoside AR agonists was not recapitulated in adenine AR antagonists, and modeling suggested an alternative, inverted binding mode with the key N250$^{6.55}$ H-bonding to the adenine N^3 and N^9, instead of N^6 and N^7 as in adenosine agonists.

Introduction

The adenosine receptors (ARs) have been developed as diverse drug targets with the envisioned therapeutic use of both agonists and antagonists.[1] Structural features and ligand recognition of the four AR subtypes (A_1, A_{2A}, A_{2B} and A_3) have been elucidated with the cumulative knowledge of structure–activity relationships (SAR), site-directed mutagenesis, computational modeling and X-ray crystallography.[2–9] In the A_{2A}AR orthosteric binding site there is an overlay of the adenine moiety of nucleosides agonists and the heterocyclic core of the most commonly co-crystallized non-purine antagonist, 4-[2-[7-amino-2-(2-furyl)-1,2,4-triazolo[1,5-*a*][1,3,5]triazin-5-yl-amino]ethyl]phenol (ZM241385), with the 5-membered and 6-membered rings of each ligand class aligned.[2–4] C2 and N^6-derivatized adenine derivatives, lacking a complete ribose-like moiety, tend to bind to the ARs as antagonists,[10–14] in some cases with similar selectivity as the corresponding adenosine derivatives, although with weaker affinity.[5] Thus, a correspondence between the positions in the agonist and antagonist series of the adenine moiety and its substituents has been predicted. We have tested that assumption through the design of novel adenine derivatives as AR antagonists, in which we examine the AR selectivity induced by previously reported agonist potency-enhancing C2 and N^6 substituents.[15–18]

N^6-Substituted adenine derivatives, such as WRC-0571 **1** (Chart 1A),[13] have been reported to be A_1AR-selective antagonists, and other adenine derivatives are selective for the A_3AR, such as 2-phenoxy-6-(cyclohexylamino)purine.[10–12,14] Previously, 2- and 8-alkynyl, 8-bromo-9-alkyl, and 8-furyl derivatives of adenine were found to bind at A_{2A}AR and other ARs.[12,19–21] A N^9-propargyl group was found to be important for the A_{2A}AR affinity of a series of 8-substituted 2-alkynyl adenine derivatives.[22]

For pharmacological studies of ARs and their modulators in human tissues and cells, the need arose to design additional A_3AR-selective antagonists or mixed antagonists of the A_1 and A_3ARs that have little or no affinity at the A_{2A} and A_{2B}-ARs.[23–25] Our approach was to combine various known A_1AR and A_3AR affinity-enhancing C2 and N^6 substituents to an adenine scaffold to modulate affinity. By analogy, various N^6-cycloalkyl and bicycloalkyl groups in adenosine derivatives are known to promote high agonist affinity at the A_1AR.[15–18,26] Furthermore, extension of the adenine C2 position in

[a] *Molecular Recognition Section, Laboratory of Bioorganic Chemistry, National Institute of Diabetes and Digestive and Kidney Diseases, National Institutes of Health, Bldg. 8A, Rm. B1A-19, NIH, NIDDK, LBC, Bethesda, Maryland, 20892-0810, USA. E-mail: kennethj@niddk.nih.gov; Fax: +301 480 8422; Tel: +301 496 9024*

[b] *School of Pharmacy, Queen's University Belfast, 96 Lisburn Rd, Belfast, BT9 7BL, UK*

[c] *Department of Pharmacology, Medical College of Wisconsin, 8701 Watertown Plank Road, Milwaukee, Wisconsin 53226, USA*

† Electronic supplementary information (ESI) available: Containing NMR and mass spectra, HPLC analysis, pharmacological studies, off-target screening and additional molecular modeling procedures/results, including MD video of **17** binding to hA_3AR. See DOI: 10.1039/c8md00317c

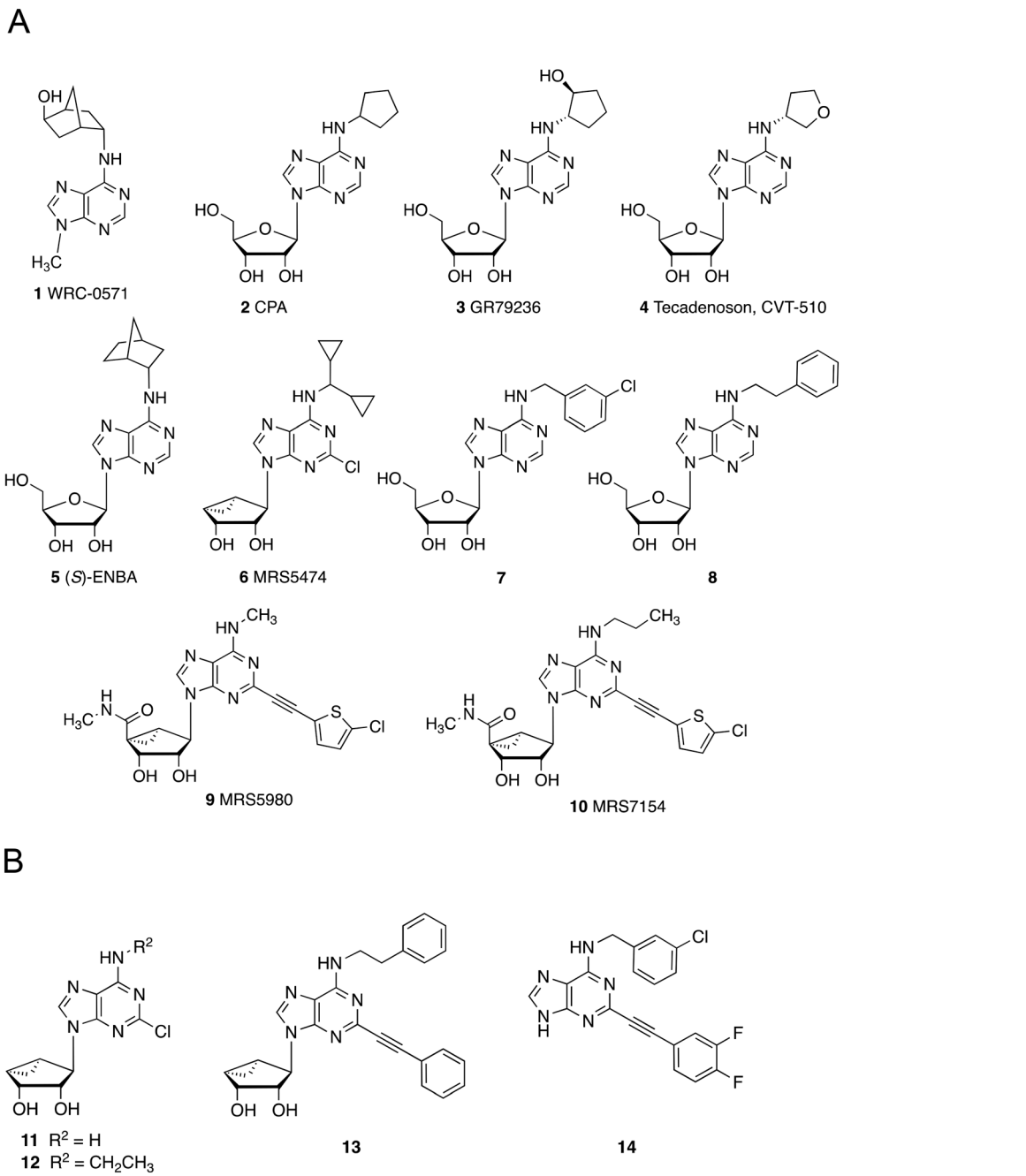

Chart 1 A. Potent AR ligands on which the selection of N^6 groups was based, including A_1AR-selective antagonist **1** and agonists **2**–**6**, and A_3AR ligands **7**–**10**. B. Truncated nucleoside analogues **11**–**14** that to illustrate that A_3AR-selectivity could be maintained by modification of the ribose ring of agonists.

adenosine derivatives with rigid arylalkynyl groups is reported to increase the affinity and selectivity of agonists at the A_3AR.[27–30] The latter selectivity was consistent with a hybrid homology model of the A_3AR in which TM2 was displaced outward to accommodate the C2 extension.[28–30] A_2AR subtypes would not be expected to undergo this outward movement of TM2 because of disulfide bridge restraints in the extracellular loop (EL) regions. We probed the compatibility of these two classes of substituents in adenine derivatives in the binding sites of both A_1 and A_3ARs, to potentially induce a mixed antagonist selectivity for these two subtypes. Previously, the combination of A_1AR-favoring N^6-cycloalkyl groups with A_3AR-favoring (*N*)-methanocarba ([3.1.0]bicyclohexane) rings in place of ribose did provide mixed agonist selectivity at these two receptors.[31] However, the combination of A_1AR-favoring N^6-cycloalkyl and A_3AR-favoring C2 substituents has not previously been explored in the adenine series.

The groups selected for the C6 position in this series of adenines are based on the following agonist substitutions (reference compounds, Chart 1A): cyclopentylamine (**2**);[32]

(1*S*,2*S*)-2-aminocyclopentan-1-ol (**3**);[33] (*R*)-tetrahydrofuran-3-amine (**4**); (1*R*,2*S*,4*S*)-bicyclo[2.2.1]heptan-2-amine (**5**, preferred isomer at A_1AR);[15,17] dicyclopropylmethylamine (**6**);[18] 3-chlorobenzylamine (**7**);[17] 2-phenylethylamine (**8**).[17] Most of these nucleoside derivatives were reported to have some degree of selectivity for A_1AR alone (**2–5**)[15–18] or mixed A_1AR/A_3AR selectivity (**7**).[31] Compound **8** was a nonselective A_1AR/A_{2A}AR/A_3AR agonist (rat) or a mixed A_1AR/A_3AR (h) ligand.[5,17] As C2 substituents, 5-chlorothien-2-ylethynyl (optimized for agonist interaction with A_3AR, *e.g.* **9** and **10**), other arylethynyl, such as *p*-sulfo-phenylethynyl (optimized for agonist interaction with A_1AR and A_3AR),[29] and propynyl were selected.

The 4′-truncated nucleosides **11–13** (Chart 1B) are included as moderately potent (K_i values 6.6–160 nM, Table 1) and selective hA_3AR reference compounds because they are intermediate between agonist structures and the target adenine derivatives. Reference hA_3AR antagonist **14** (K_i value 120 nM) combines several of the above-mentioned features in an adenine derivative.[5] 4′-Truncated (*N*)-methanocarba nucleosides derived from A_3AR-selective agonists, *e.g.* **11–13**, typically bind to the receptor as low efficacy partial agonists or antagonists. The maximal efficacy of **13** to activate A_3AR-mediated inhibition of cAMP formation was only 4.1 ± 1.2% (h) and 14.3 ± 6.1% (m).[29] Compounds **12** and **13** were included to illustrate that A_3AR-selectivity could be maintained with a residual, incomplete pseudoribose moiety anchoring the adenine moiety in the binding site. Nonselective compound **11** was also a partial agonist at hA_1AR; it activated A_1AR-mediated inhibition of cAMP formation with a 68% maximal efficacy.[18] Thus, the target adenine antagonists contained hybrid features of A_1AR and A_3AR ligands.

Results and discussion

Chemical synthesis

The synthesis of fifteen novel, but related adenine derivatives (**15–29**, Table 1) was performed as shown in Scheme 1. The target adenines contained either H or CH_3 at the N^9 position, various N^9-aryl/alkyl or cycloalkyl substitutions and extended C2 groups, identical or similar to **9** and **10**.

Commercially available 6-chloro-2-iodopurine **35** was selectively protected with a THP group or methylated by iodomethane at N^9 position to give **36a** or **36b**. The palladium-catalyzed condensation of compounds **36a–b** with 2-chloro-5-ethynylthiophene yielded **37a–b**, followed by removal of the THP group of **37a** under acidic condition to afford **37c**. Compounds **37b–c** were treated with various amines to give C2, N^6-substituted adenine derivatives **15–27**.

Since N^6-dicyclopropylmethyl analogue **22** exhibited moderate 32-fold A_3AR binding selectivity compared to A_1AR (see SAR analysis below and Table 1), other C2-modified-N^6-dicyclopropylmethyl-adenines were prepared. The amination of 6-chloro-2-iodopurine with dicyclopropylmethylamine gave **38**, which was condensed with a monosubstituted alkyne using a Sonogashira coupling to afford **28–29**. 2-(2-Chlorothien-5-yl)-N^6-cyclopentyl derivative **18** was also obtained by an analogous route *via* the 2-iodo-adenine intermediate **39**.

SAR analysis

The structure activity relationship (SAR) of N^6 and C2 substituted adenines was explored. The initial biological characterization consisted of standard radioligand binding assays at human (h) A_1AR/A_{2A}AR/A_3AR using compounds **31–34** (footnote a, Table 1), performed as described.[14,17,18] IC_{50} values were converted to K_i values as reported.[34] Reference compounds with similar N^6 substituents (adenosine derivatives **2–5**, **7** and **8**; truncated (*N*)-methanocarba nucleosides **6** and **11–13**; adenine derivative **14**) that were already reported to bind with various degrees of AR affinity and selectivity are shown in Table 1 for comparison.

Among the adenine derivatives, moderate hA_3AR affinity was observed for **14**,[5] which suggested that this affinity might be enhanced by N^6 and C2 modification. Small N^6-alkyl groups enhance hA_3AR agonist affinity, and the C2-chlorothienylethynyl group is suited for a long duration of A_3AR agonist action.[35] Consistently, these modifications of adenine in **15–17** produced hA_3AR selectivity, with an affinity (K_i, nM) order of: *n*-Pr (16) > Et (33) > Me (79) at N^6. Compounds **18–22** contain substituents that are both A_1AR and A_3AR-enhancing in agonists, but these adenine derivatives were predominantly A_3AR selective, with K_i values in the range of 12–37 nM. hA_3AR-selective N^6-propyl derivative **17** (~1000-fold compared to A_1AR and A_{2A}AR, K_i 16.4 nM) is a truncated analogue of potent and selective A_3AR agonist **10**. Compound **17** displays 15-fold lower hA_3AR binding affinity than **10** and no difference in the lack of A_1AR and A_{2A}AR affinity. The ligand efficiency (LE) of **17** is a favorable 0.519, its clog*P* is 3.29, and its predicted intestinal absorption and fraction unbound (human) are 90% and 37%, respectively.[36]

Thus, we have enhanced the robust A_3AR-preferring pharmacological profile of the initial adenine lead **14**, despite the presence of diverse A_1AR-enhancing groups at N^6. N^6 groups that in agonists are either A_3AR-preferring (**23**, 3-halobenzyl, K_i 128 nM) or affinity-enhancing at multiple subtypes (**24**, 2-phenylethyl) did not increase the A_3AR selectivity compared to **14**. Curiously, the potent hA_3AR binding of this N^6-2-phenylethyl analogue (**24**, K_i 13 nM) was abolished by 3,4-dihydroxy (**25**) or by 4-hydroxy-3-methoxy (**26**) substitution of the phenyl ring (K_i > 10 and 6.8 μM, respectively).

Previous study of the selectivity of adenine derivatives at the A_3AR indicated that 9-H favored higher affinity compared to a 9-methyl or 9-ethyl substitution,[5,14] although an adenine 9-Me group improved A_{2A}AR affinity.[37] One compound, **27**, contained a 9-methyl substitution in order to test the generality of this observation. Compound **27** displayed a K_i value at hA_3AR of 116 nM, showing an 8.9-fold reduction of the high hA_3AR affinity (K_i 13 nM) of corresponding 9-H derivative **24**, and a 2.8-fold reduction of its weak hA_1AR affinity (K_i 1.75 μM) of **24**, thus confirming the generality of this 9-alkyl substitution as disfavoring AR affinity in the adenine series of

Table 1 Structures and binding affinities (in human, unless noted) of adenosine and adenine derivatives as AR ligands, determined in binding assays performed as reported. [a] Reference compounds **1**–**14** were included for comparison. Unless noted, R^3 = H

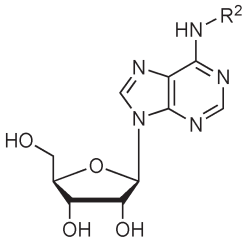

2–5, 7, 8

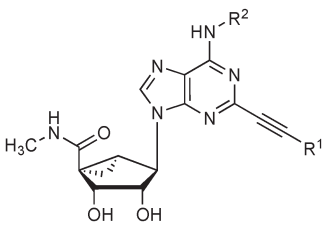

9, 10

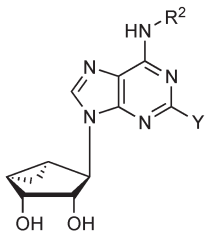

6, 11–13

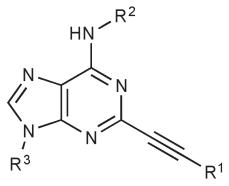

14–29

Compound, other substitution	R^1 (or Y)	R^2	A_1AR % inhibition or K_i[a] (nM)	A_{2A}AR % inhibition or K_i[a] (nM)	A_3AR % inhibition or K_i[a] (nM)
Reference AR ligands[b,c]					
2	—	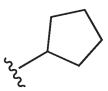	2.3	794	72
3	—	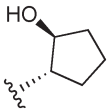	3.89 ± 0.59, 3.1 (r)	1330	ND
4	—	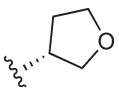	6.5 (p)	2315	ND
5	—		0.38 ± 0.19, 0.34 ± 0.06 (r)	>10 000, 477 ± 72 (r)	915 ± 299, 282 ± 101 (r)
6	Y = Cl	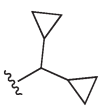	47.9 ± 10.5	3950 ± 410	470 ± 15
7	—	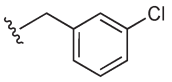	45 ± 10 (r)	>10 000 (r)	4.4 ± 1.7, 35 ± 20 (r)
8	—	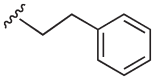	12.9, 24 ± 8 (r)	676, 161 (r)	2.1 ± 0.4, 240 ± 58 (r)
9	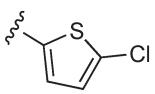	CH_3	*<10%*	*24 ± 13%*	0.70 ± 0.11, 36 ± 5 (m)
10	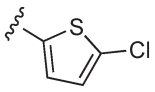	$(CH_2)_2CH_3$	*22 ± 5%*	*34 ± 3%*	1.1 ± 0.3, 6.8 ± 0.3 (m)
11	Y = Cl	H	350 ± 90	3140 ± 450	160 ± 42
12	Y = Cl	CH_2CH_3	930 ± 110	*11%*	6.6 ± 1.6
13	Y = 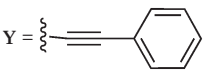	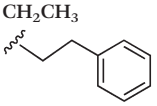	*30 ± 8%, 39 ± 6%* (m)	*22 ± 5%, 13 ± 2%* (m)	20.0 ± 6.0, 480 ± 90 (m)
14	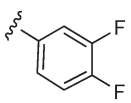	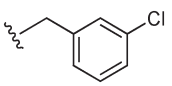	*<10%*	*<10%*	120 ± 17
Novel adenine derivatives[c]					
15	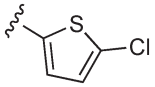	CH_3	*25 ± 8%*	1330 ± 450	79.2 ± 21.9

Table 1 *(continued)*

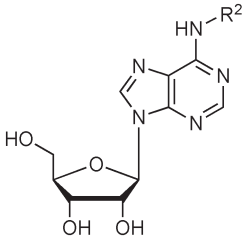

2–5, 7, 8

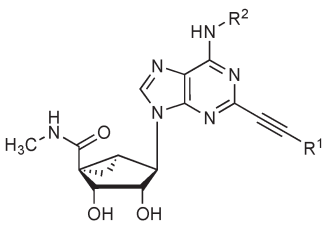

9, 10

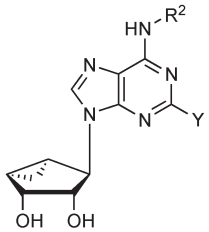

6, 11–13

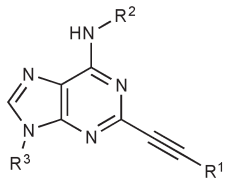

14–29

Compound, other substitution	R^1 (or Y)	R^2	A_1AR % inhibition or K_i^a (nM)	$A_{2A}AR$ % inhibition or K_i^a (nM)	A_3AR % inhibition or K_i^a (nM)
16	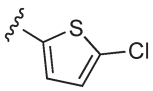	CH_2CH_3	*32 ± 1%*	*18 ± 2%*	33.1 ± 8.0
17	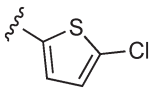	$(CH_2)_2CH_3$	*31 ± 7%*	*25 ± 7%*	16.4 ± 2.5, *27 ± 3%* (m)
18	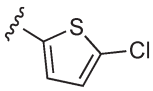	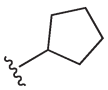	1120 ± 320	1340 ± 540	17.4 ± 2.8
19	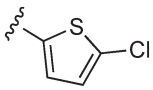	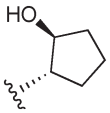	1490 ± 380	7070 ± 1430	11.7 ± 2.9
20	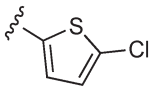	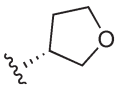	687 ± 538	2370 ± 770	32.0 ± 3.8, *20 ± 1%* (m)
21	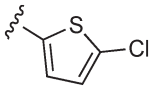		1050 ± 490	*37 ± 13%*	20.6 ± 4.4
22	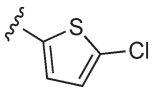	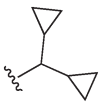	1200 ± 180	*6 ± 2%*	37.1 ± 6.0
23	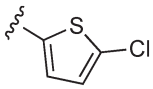	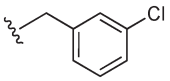	2710 ± 1950	*1 ± 3%*	128 ± 8
24	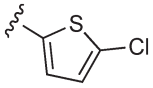	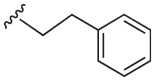	1750 ± 290	*21 ± 1%*	13.0 ± 2.6, *7 ± 1%* (m)
25	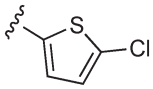	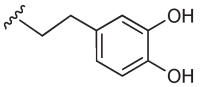	*28 ± 5%*	*5 ± 2%*	*20 ± 2%*
26	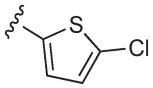	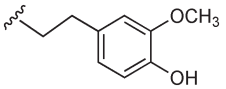	*15 ± 4%*	*−3 ± 2%*	6820 ± 2010
27, $R^3 = CH_3$	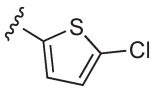	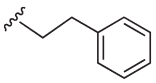	4850 ± 2990	*32 ± 11%*	116 ± 7, *16 ± 2%* (m)
28	CH_3	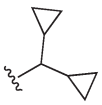	2870 ± 870	3240 ± 520	43.2 ± 7.1

Table 1 *(continued)*

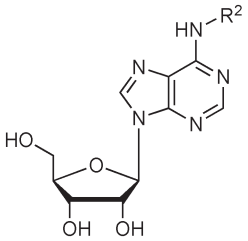

2–5, 7, 8

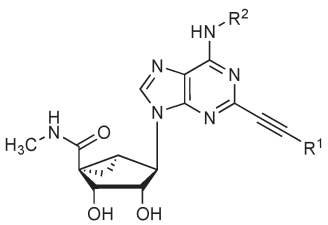

9, 10

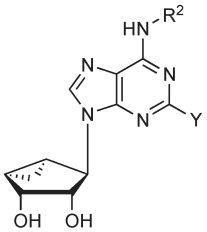

6, 11–13

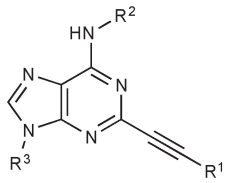

14–29

Compound, other substitution	R^1 (or Y)	R^2	A_1AR % inhibition or K_i[a] (nM)	A_{2A}AR % inhibition or K_i[a] (nM)	A_3AR % inhibition or K_i[a] (nM)
29	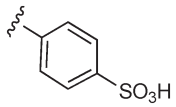	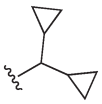	*54 ± 7%*	*21 ± 2%*	*26 ± 6%*

[a] Binding in membranes of HEK293 (hA_{2A} and mA_3) and CHO (hA_1 and hA_3) cells stably expressing one of three hAR subtypes, unless noted. The binding affinity at mA_3AR was determined as reported using adenosine-5′-*N*-ethyluronamide (NECA, 10 μM) **30** to determine nonspecific binding.[29] The binding affinity for hA_1, hA_{2A} and A_3ARs was expressed as K_i values using agonists [^{3}H]8-cyclopentyl-1,3-dipropylxanthine (DPCPX, 0.5 nM) **31**, [^{3}H]4-[2-[7-amino-2-(2-furyl)-1,2,4-triazolo[1,5-a][1,3,5]triazin-5-yl-amino]ethyl]phenol (ZM241385, 1 nM) **32**, or [^{125}I]*N*^{6}-(4-amino-3-iodobenzyl)-adenosine-5′-*N*-methyluronamide (I-AB-MECA, 0.1 nM) **33**, respectively. Nonspecific binding was determined using *N*-(2-aminoethyl)-2-[4-(2,3,6,7-tetrahydro-2,6-dioxo-1,3-dipropyl-1*H*-purin-8-yl)phenoxy]-acetamide (XAC) **34** (10 μM). Values are expressed as the mean ± SEM (n = 3, unless noted). K_i values were calculated as reported.[34] A percent in italics refers to inhibition of specific radioligand binding at 10 μM. Compounds **15**, **17**, **24** and **28** (10 μM) were shown to not bind appreciably at the hA_{2B}AR (see text). The cell lines were from American Type Culture Collection (ATCC, Manassas, VA), and the cDNA for the ARs was obtained from cdna.org. [b] Data from Jacobson *et al.*,[5] Gao *et al.*,[17] Tosh *et al.*,[18,28,30,35,44] and Paoletta *et al.*[29] [c] **1**, WRC-0571; **3**, GR79236X; **4**, tecadenoson, CVT-510; **5**, *S*-ENBA; **9**, MRS5980; **10**, MRS7154; **17**, MRS7497; **19**, MRS7326; **24**, MRS7350.

antagonists. The N^9-methyl group also reduced the predicted free fraction (human) from 22% for **24** to 4.6% for **27**.[36]

Shortening the terminal group on the C2-alkyne from aryl to methyl was slightly permissive for A_{2A}AR (K_i 3.24 μM) in **28** (*cf.* **22**) with only minor changes in A_1AR and A_3AR affinity (K_i 2.87 μM and 43 nM, respectively). However, a C2-terminal *p*-sulfophenyl group, as in **29**, was compatible with both high A_1AR and A_3AR affinity in the agonist series,[29] but eliminated this binding in the adenine series with K_i values ≥ 10 μM at both subtypes.

AR antagonists of mixed A_1 and A_3AR selectivity to the exclusion of A_{2A} and A_{2B}ARs have also been predicted to be useful in diabetic models.[17] We included this goal in our initial design of the target adenine derivatives, but this approach was not suitable for designing adenine antagonists with that mixed selectivity. Selective A_3AR antagonists have potential utility in glaucoma, kidney protection, inflammatory conditions and cancer.[38,39] Some of the adenine derivatives show clear selectivity for the hA_3AR, but none are balanced between A_1 and A_3ARs. Furthermore, they are not useful as pharmacological probes of the mouse (m) A_3AR. The truncated derivative **13** was previously shown to lose A_3AR affinity between the two species by a factor of 24-fold,[29] and the ratio for species-dependence of the adenine derivatives was estimated as >1000-fold for **24** and other analogues for which no significant binding at mA_3AR was determined, *i.e.* **17**, **20** and **27**. Thus, the affinity in this adenine series was highly species-dependent, as illustrated by the inactivity of representative compounds **17**, **20**, **24** and **27** at the mA_3AR.

Additional pharmacological experiments were performed to establish that these derivatives are selective hA_3AR antagonists. Four representative adenine derivatives were found to lack affinity in a hA_{2B}AR binding assay in HEK cell membranes overexpressing the receptor, using as radioligand xanthine antagonist [^{3}H]MRS1754, performed as reported.[40] The percent inhibition of specific binding at 10 μM was: **15**, 6.2 ± 1.0%; **17**, 10.4 ± 6.1%; **24**, −10.4 ± 6.1%; **28**, 22.7 ± 5.0%. Although there is no precedent for an adenine derivative (non-riboside analogue) activating ARs, we nevertheless tested representative adenine derivative **18** (binding K_i 17.4 nM) in a functional assay of hA_3AR-induced cAMP accumulation induced by the non-selective agonist NECA **30**.[41] The agonist activation curve was right-shifted (Fig. 1), indicating potent hA_3AR antagonism consistent with its binding affinity.

Off-target interactions with other receptors and ion channels were determined by the PDSP (ESI†).[42] There were only limited weak off-target interactions, noted at the following receptors (K_i, μM): **13**, σ_2 1.30 (h), NET 2.80; **16**, D_1 5.11; σ_1 1.16; **17**, σ_1 1.52, σ_2 1.91; **18**, α_{2C} 1.49; **19**, $5HT_{2B}$ 1.86, $5HT_{2C}$ 1.10; **20**, M_4 1.74; **21**, H_2 3.64; **22**, TSPO 2.02; **23**, α_{2B} 1.72, σ_2 0.90; **24**, $5HT_{2C}$ 1.19, H_2 0.52; **25**, $5HT_{2B}$ 1.21, α_{2C} 3.52; **26**, σ_1 1.39, σ_2 0.37; **27**, TSPO 3.17. **28** and **29** were not tested for off-target activity.

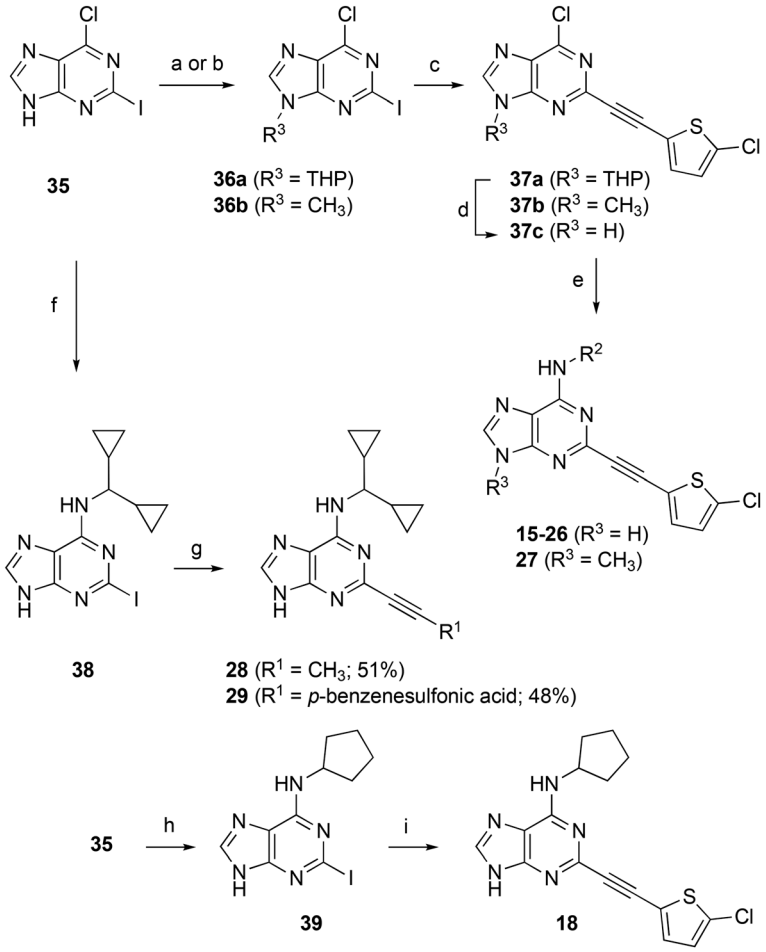

Scheme 1 Synthesis of adenine derivatives as AR antagonists. Reagents and conditions: a) DHP, TsOH, THF, rt, 16 h for **36a**, 96%; b) CH_3I, K_2CO_3, DMF, rt, 1 h for **36b**, 70%; c) 2-Cl-5-ethynylthiophene, $PdCl_2(PPh_3)_2$, CuI, Et_3N, dioxane, rt, 1 h, 82–99%; d) TFA : DCM = 1 : 9, rt, 2 h, 88%; e) amine, Et_3N or DIPEA, EtOH, reflux (method A) or μW (method B), 57–93%; f) dicyclopropylmethylamine·HCl, DIPEA, iPrOH, μW, 90 °C, 3 h, 97%; g) propyne (for **28**; 51%) or 4-ethynylbenzenesulfonic acid (for **29**; 48%), $PdCl_2(PPh_3)_2$, CuI, Et_3N, DMF; h) cyclopentylamine, Et_3N, EtOH, reflux, 15 h, 48%; i) 2-Cl-5-ethynylthiophene, $PdCl_2(PPh_3)_2$, CuI, Et_3N, DMF, 70 °C, 2 h, 47% (method C).

Computational studies

The interaction of 9-alkyladenine derivatives with the $hA_{2A}AR$ has already been modeled using docking[12] and molecular dynamics (MD) free energy calculations,[36] and the adenine moiety was coordinated with a binding mode similar to adenosine agonists. Molecular recognition of the newly synthesized derivatives (**15–29**) was predicted using a hA_3AR homology model based on a high-resolution X-ray structure of the hA_{2A}-AR in the inactive conformation (PDB ID: 4EIY). A more in-depth MD analysis was carried out for the most selective adenine derivative **17** (N^9 unsubstituted), that could be considered a pseudoribose-truncated analogue of the potent A_3AR agonist **10**.[36] Surprisingly, the modeling analysis did not support the initial assumption of adenine derivatives bearing a C2 extension binding in the same orientation hypothesized for adenosine agonists. The docking poses of the adenine antagonists, indeed, featured the extended C2 substituent pointing downwards into the A_3AR ribose-binding subpocket, rather than toward TM2.

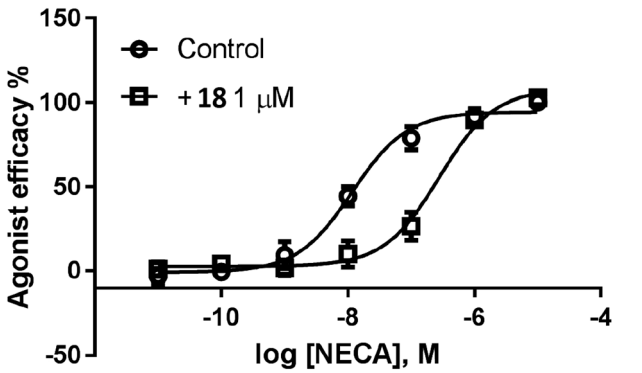

Fig. 1 Representative adenine derivative **18** antagonizes the effects of non-selective AR agonist NECA **30** in a functional assay of hA_3AR-induced cAMP accumulation in CHO cells, performed as reported.[41] The EC_{50} values (nM) were: NECA alone, 11.7; +**18**, 276.

In Fig. 2A, the most favorable docking pose of **17** is reported as an example; for the sake of comparison, the

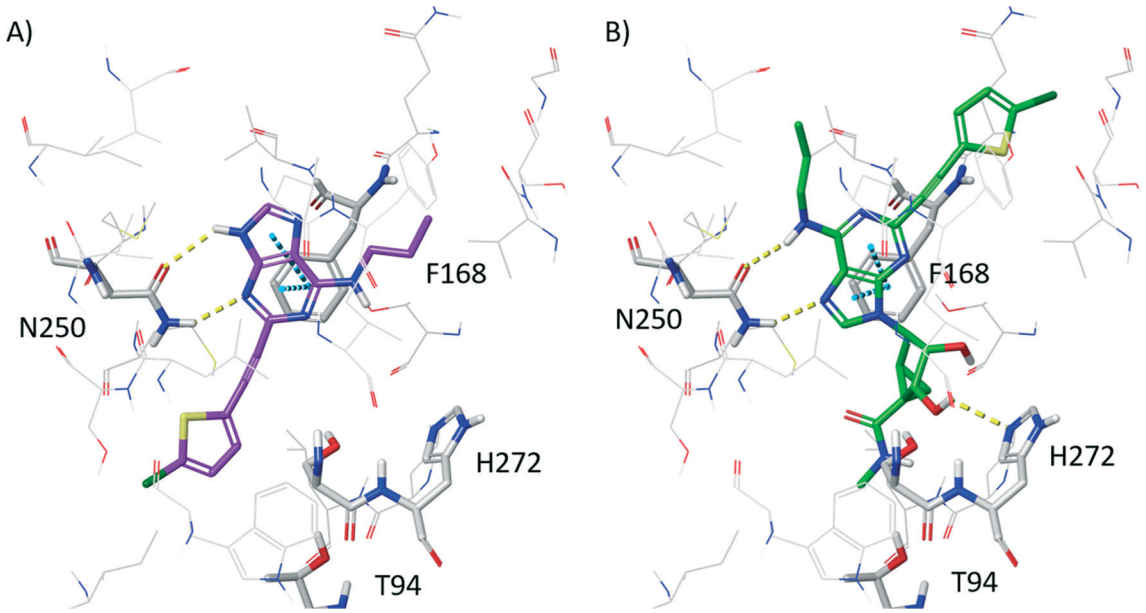

Fig. 2 Docking of **17** (A) and **10** (B) at the inactive hA_3AR homology model, using as template an $A_{2A}AR$ inactive structure (PDB ID: 4EIY). The antagonist **17** is docked with the C2 group pointing down in the TM bundle and toward the TM4/TM5 interface. The pose of **17** following MD simulation is stable and reproducible. The orientation of the adenine scaffold is consistent with the existence of two hydrophobic pockets, one at the interface of TMs 4–6 and another at the interface of TMs 1–3. The shift of TM2 in (B, cyan arrow) allows the scaffold of agonist **10** to sit deeper in the binding site and reach Thr94.

docking pose of **10** at the hA_3AR inactive model is shown in Fig. 2B. The adenine moiety of **17** was coordinated by the conserved $N250^{6.55}$ (residue numbers are given according to a standard convention[43]) with its N^9-H and N^3, rather than the coordination with N^6-H and N^7 as seen with agonist **10**. As shown in Fig. S1,† the adenine cores of the two ligands when superimposed did not overlap, because the orientation of **17** was reversed with respect to the orientation predicted for the agonist **10**. However, the parallel in A_3AR SAR between the adenine and adenosine series would predict an overlay. Therefore, we carried out MD simulation of the **17**-hA_3AR complex starting from two different binding modes: the most favorable docking pose showed in Fig. 2A (hereby denoted as BM1), and a conformation derived by removing the methanocarba ring from the pose predicted for **10** (hereby denoted as BM2, Fig. S2†). We then subjected the two ligand–protein complexes to 30 ns of MD simulation (run in triplicate). As suggested by the RMSD values reported in Table S1,† BM2 was not stable (average ligand RMSD = 4.07 ± 1.77 Å). An inspection of the trajectories revealed that the scaffold turned during the equilibration phase and pointed the C2 extension toward the EC environment. On the other hand, BM1 was stable over time (average ligand RMSD = 1.79 ± 0.31 Å) and featured strong and persistent ligand–protein interactions. As visualized in Video S1† (selected run2), the adenine core of **17** engaged in π–π stacking interaction with the side chain of $F168^{EL2}$ and established hydrophobic contacts with $L246^{6.51}$ and $L264^{7.35}$ and a H-bond with $N250^{6.55}$ that was partly water-mediated. The C2 extension was hosted in a hydrophobic cavity the interface between TM5 and TM6 surrounded by aromatic and hydrophobic residues, including $F182^{5.43}$, $I186^{5.47}$, $I98^{3.40}$, $F239^{6.44}$, $W243^{6.48}$, and $M177^{5.38}$. The N^6-propyl substitution pointed toward TM2 and established hydrophobic interactions with $I268^{7.39}$ and $L90^{3.32}$ residues.

The A_3AR selectivity of C2-arylalkynyl adenosines has been proposed to be a result of the multiple disulfide bonds of the ELs constraining TM2 in the $A_{2A}AR$. Evidently, the C2 rigid extension does not permit A_1AR binding, both in the A_3AR agonist series[28–30] and in the adenine series. The explanation for lack of affinity of the extended C2-arylalkynyl adenines at the A_1AR and the $A_{2A}AR$, however, might rely on the different size of the pocket predicted to host the C2 group, which for the adenines lies at the interface between TM5 and TM6. As depicted in Fig. 3, the superimposition of the docking pose of **17** at the A_3AR homology model (magenta carbon sticks) with the A_1 and the A_{2A} (grey and green carbon sticks, respectively) AR inactive X-ray structures highlighted, along with the well-known differences in residues at the interface between EL2 and TM7, remarkable differences in the size and properties of residues located at the $X^{5.47}$ and $X^{6.52}$ positions surrounding the 2-chloro-thienyl moiety. In the A_3AR model, the presence of a serine residue ($S247^{6.52}$) in place of a His enlarges the cavity hosting the C2 terminal aromatic ring and the presence of a bulkier isoleucine side chain ($I186^{5.47}$) in place of a Val enables additional hydrophobic contacts with the ligand.

Experimental section

Chemistry

Materials and instrumentation. Most reagents and solvents were purchased from Sigma-Aldrich (St. Louis, MO).

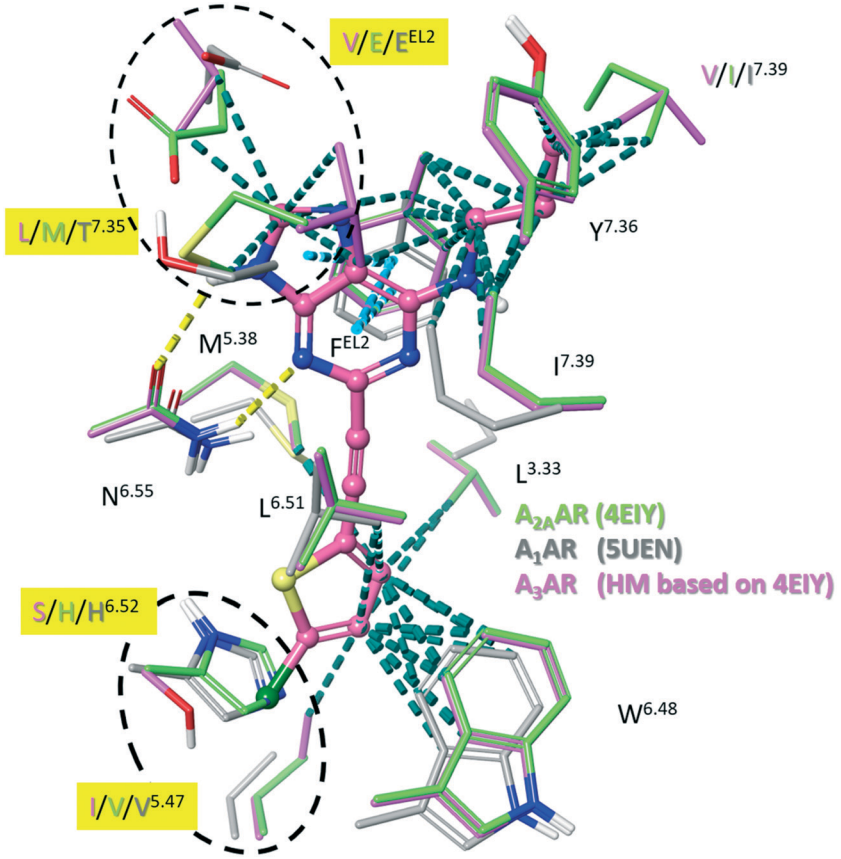

Fig. 3 Superimposition of the docking pose of **17** (balls and sticks, magenta carbon atoms) at the inactive hA_3AR homology model (sticks, magenta carbon atoms) with the $A_{2A}AR$ (PDB ID: 4EIY, sticks with green carbon atoms) and A_1AR (PBD ID: 5UEN, sticks with grey carbon atoms) inactive structures. Regions with differing residues (highlighted in yellow) are indicated with black circles (dashes lines). In the docking pose H-bond, π–π stacking, and hydrophobic interactions are depicted as yellow, cyan, and dark green dashed lines, respectively.

Compound **35** was from Astatech (Bristol, PA), and potassium 4-iodobenzenesulfonate was purchased from Matrix Scientific, Inc. (Columbia, SC). ^{1}H NMR spectra were obtained with a Bruker 400 spectrometer using $CDCl_3$, CD_3OD, and DMSO-d_6 as solvents. Chemical shifts are expressed in δ values (ppm) with tetramethylsilane (δ 0.00) for $CDCl_3$ and water (δ 3.30) for CD_3OD. NMR spectra were collected with a Bruker AV spectrometer equipped with a *z*-gradient [^{1}H,^{13}C,^{15}N]-cryoprobe. TLC analysis was carried out on glass sheets precoated with silica gel F254 (0.2 mm) from Sigma-Aldrich. Low-resolution mass spectrometry was performed with a JEOL SX102 spectrometer with 6 kV Xe atoms following desorption from a glycerol matrix or on an Agilent LC/MS 1100 MSD, with a Waters (Milford, MA) Atlantis C18 column. High resolution mass spectroscopic (HRMS) measurements were performed on a proteomics optimized Q-TOF-2 (Micromass Waters) using external calibration with polyalanine, unless noted. Observed mass accuracies are those expected based on known performance of the instrument as well as trends in masses of standard compounds observed at intervals during the series of measurements. Reported masses are observed masses uncorrected for this time dependent drift in mass accuracy.

General procedure for 15–27

Method A. To a solution of compound **37b–c** (1 eq) and amine (2 eq) in ethanol was added triethylamine (2 eq) at room temperature, and the reaction mixture was refluxed for 1 d to 3 d. After all volatiles were evaporated under reduced pressure, the crude was purified by silica gel column chromatography (dichloromethane : methanol = 50 : 1).

Method B. To a solution of compound **37c** (1 eq) and amine (5 eq) in ethanol was added *N*,*N*-diisopropylethylamine (10 eq) at room temperature, and the reaction mixture was heated in microwave synthesizer (Biotage Initiator, Biotage, Charlotte, NC) at 90 °C for 1 h. After all volatiles were evaporated under reduced pressure, the crude was purified by silica gel column chromatography (dichloromethane : methanol = 50 : 1).

2-((5-Chlorothiophen-2-yl)ethynyl)-*N*-methyl-9*H*-purin-6-amine (15). Method B; yield: 83%; ^{1}H NMR (400 MHz, DMSO-d_6) δ 8.16 (s, 1H), 7.77 (s, 1H), 7.44 (s, 1H), 7.22 (d, J = 3.36 Hz, 1H), 2.98 (s, 3H); MS (ESI, *M*/*Z*) 290.0, 292.0 [M + H]$^+$; ESI-HRMS calcd for $C_{12}H_9N_5{}^{32}S^{35}Cl$ 290.0267, found 290.0265 [M + H]$^+$.

2-((5-Chlorothiophen-2-yl)ethynyl)-*N*-ethyl-9*H*-purin-6-amine (16). Method B; yield: 92%; ^{1}H NMR (400 MHz,

CD_3OD) δ 8.10 (s, 1H), 7.32 (d, J = 3.84 Hz, 1H), 7.02 (d, J = 3.88 Hz, 1H), 3.67 (broad s, 2H), 1.33 (t, J = 7.18 Hz, 3H); MS (ESI, M/Z) 304.0, 306.0 $[M + H]^+$; ESI-HRMS calcd for $C_{13}H_{11}N_5{}^{32}S^{35}Cl$ 304.0424, found 304.0422 $[M + H]^+$.

2-((5-Chlorothiophen-2-yl)ethynyl)-*N*-propyl-9*H*-purin-6-amine (17). Method B; yield: 62%; ^{1}H NMR (400 MHz, CD_3-OD) δ 8.11 (s, 1H), 7.32 (d, J = 3.88 Hz, 1H), 7.02 (d, J = 3.96 Hz, 1H), 3.61 (broad s, 2H), 1.79–1.70 (m, 2H), 1.06 (t, J = 7.40 Hz, 3H); MS (ESI, M/Z) 318.1, 320.1 $[M + H]^+$; ESI-HRMS calcd for $C_{14}H_{13}N_5{}^{32}S^{35}Cl$ 318.0580, found 318.0585 $[M + H]^+$.

2-((5-Chlorothiophen-2-yl)ethynyl)-*N*-cyclopentyl-9*H*-purin-6-amine (18). Method C: a suspension of **39** (11 mg, 33 μmol), $PdCl_2(PPh_3)_2$ (4.9 mg, 6.98 μmol), copper(I) iodide (1.8 mg, 9.45 μmol) and triethylamine (45 μl, 33 mg, 0.33 mmol) in DMF (0.5 mL) was purged with nitrogen gas for 30 min. To the reaction mixture was added a solution of 2-chloro-5-ethynylthiophene (24 mg, 0.17 mmol) in DMF (0.5 mL), and this mixture was stirred at 70 °C for 2 h. After all volatiles were evaporated under reduced pressure, and the residue was purified by silica gel chromatography (dichloromethane : methanol = 50 : 1) to afford compound **18** (5.4 mg, 47%) as a white solid.

Method B; yield: 93%; ^{1}H NMR (400 MHz, CD_3OD) δ 8.12 (s, 1H), 7.32 (d, J = 4.0 Hz, 1H), 7.02 (d, J = 4.0 Hz, 1H), 4.60 (broad s, 1H), 2.16–2.12 (m, 2H), 1.86–1.83 (m, 2H), 1.75–1.71 (m, 2H), 1.68–1.62 (m, 2H); MS (ESI, M/Z) 344.1, 346.1 $[M + H]^+$; ESI-HRMS calcd for $C_{16}H_{15}N_5{}^{32}S^{35}Cl$ 344.0737, found 344.0737 $[M + H]^+$.

(1*S*,2*S*)-2-((2-((5-Chlorothiophen-2-yl)ethynyl)-9*H*-purin-6-yl)amino)cyclopentan-1-ol (19). Method A; yield: 75%; ^{1}H NMR (400 MHz, CD_3OD) δ 8.15 (s, 1H), 7.32 (d, J = 4.0 Hz, 1H), 7.03 (d, J = 4.0 Hz, 1H), 4.34 (m, 1H), 4.16–4.12 (m, 1H), 2.36–2.30 (m, 1H), 2.11–2.06 (m, 1H), 1.93–1.83 (m, 2H), 1.75–1.68 (m, 2H); MS (ESI, M/Z) 360.0, 362.1 $[M + H]^+$; ESI-HRMS calcd for $C_{16}H_{15}N_5O^{32}S^{35}Cl$ 360.0686, found 360.0688 $[M + H]^+$.

(*R*)-2-((5-Chlorothiophen-2-yl)ethynyl)-*N*-(tetrahydrofuran-3-yl)-9*H*-purin-6-amine (20). Method A; yield: 76%; ^{1}H NMR (400 MHz, $CDCl_3$) δ 7.98 (s, 1H), 7.26 (d, J = 3.92 Hz, 1H), 6.90 (d, J = 3.96 Hz, 1H), 6.22 (broad s, 1H), 5.06 (broad s, 1H), 4.09–4.04 (m, 2H), 3.96–4.00 (m, 1H), 3.86 (dd, J = 2.94, 9.32 Hz, 1H), 2.51–2.42 (m, 1H), 2.04–2.01 (m, 1H); MS (ESI, M/Z) 346.1, 348.1 $[M + H]^+$; ESI-HRMS calcd for $C_{15}H_{13}N_5O^{32}S^{35}Cl$ 346.0529, found 346.0532 $[M + H]^+$.

***N*-((1*R*,2*S*,4*S*)-Bicyclo[2.2.1]heptan-2-yl)-2-((5-chlorothiophen-2-yl)ethynyl)-9*H*-purin-6-amine (21).** Method B; yield: 88%; ^{1}H NMR (400 MHz, CD_3OD) δ 8.12 (s, 1H), 7.32 (d, J = 4.0 Hz, 1H), 7.02 (d, J = 4.0 Hz, 1H), 4.13 (broad s, 1H), 2.37 (m, 2H), 1.98–1.92 (m, 1H), 1.67–1.53 (m, 3H), 1.49–1.41 (m, 2H), 1.32–1.25 (m, 3H); MS (ESI, M/Z) 370.1, 372.1 $[M + H]^+$; ESI-HRMS calcd for $C_{18}H_{17}N_5{}^{32}S^{35}Cl$ 370.0893, found 370.0891 $[M + H]^+$.

2-((5-Chlorothiophen-2-yl)ethynyl)-*N*-(dicyclopropylmethyl)-9*H*-purin-6-amine (22). Method A; yield: 66%; ^{1}H NMR (400 MHz, $CDCl_3$) δ 7.95 (s, 1H), 7.24 (d, J = 4.0 Hz, 1H), 6.39 (d, J = 4.0 Hz, 1H), 1.12–1.06 (m, 2H), 0.90 (t, J = 6.8 Hz, 1H), 0.59–0.42 (m, 8H); MS (ESI, M/Z) 370.1, 372.1 $[M + H]^+$; ESI-HRMS calcd for $C_{18}H_{17}N_5{}^{32}S^{35}Cl$ 370.0893, found 370.0892 $[M + H]^+$.

***N*-(3-Chlorobenzyl)-2-((5-chlorothiophen-2-yl)ethynyl)-9*H*-purin-6-amine (23).** Method A; yield: 91%; ^{1}H NMR (400 MHz, DMSO-d_6) δ 8.24 (s, 1H), 7.45–7.41 (m, 3H), 7.36–7.31 (m, 4H), 7.21 (d, J = 3.6 Hz, 1H), 4.71 (broad s, 1H); MS (ESI, M/Z) 400.0, 402.0 $[M + H]^+$; ESI-HRMS calcd for $C_{18}H_{12}N_5{}^{32}S^{35}Cl_2$ 400.0190, found 400.0196 $[M + H]^+$.

2-((5-Chlorothiophen-2-yl)ethynyl)-*N*-phenethyl-9*H*-purin-6-amine (24). Method B; yield: 70%; ^{1}H NMR (400 MHz, CD_3-OD) δ 8.10 (s, 1H), 7.33–7.19 (m, 7H), 7.03 (d, J = 3.96 Hz, 1H), 3.91 (broad s, 1H), 3.03 (t, J = 7.24 Hz, 2H); MS (ESI, M/Z) 380.1, 382.1 $[M + H]^+$; ESI-HRMS calcd for $C_{19}H_{15}N_5{}^{32}S^{35}Cl$ 380.0737, found 380.0739 $[M + H]^+$.

2-((5-Chlorothiophen-2-yl)ethynyl)-*N*-(3,4-dihydroxyphenethyl)-9*H*-purin-6-amine (25). Method A; yield 57%: ^{1}H NMR (400 MHz, CD_3OD) δ 8.10 (s, 1H), 7.33 (broad s, 1H), 7.02 (broad s, 1H), 6.73–6.69 (m, 2H), 6.64–6.60 (m, 1H), 3.38–3.30 (m, 2H), 2.88–2.84 (m, 2H); MS (ESI, M/Z) 412.1, 414.1 $[M + H]^+$; ESI-HRMS calcd for $C_{19}H_{15}N_5O_2{}^{32}S^{35}Cl$ 412.0635, found 412.0632 $[M + H]^+$.

2-((5-Chlorothiophen-2-yl)ethynyl)-*N*-(4-hydroxy-3-methoxyphenethyl)-9*H*-purin-6-amine (26). Method A; yield 63%: ^{1}H NMR (400 MHz, CD_3OD) δ 8.18 (s, 1H), 7.33 (d, J = 3.80 Hz, 1H), 7.03 (d, J = 3.84 Hz, 1H), 6.89 (s, 1H), 6.72 (s, 2H), 3.86 (s, 3H), 3.34–3.30 (m, 2H), 2.93 (t, J = 6.88 Hz, 2H); MS (ESI, M/Z) 426.1, 428.1 $[M + H]^+$; ESI-HRMS calcd for $C_{20}H_{17}N_5O_2{}^{32}S^{35}Cl$ 426.0791, found 426.0792 $[M + H]^+$.

2-((5-Chlorothiophen-2-yl)ethynyl)-9-methyl-*N*-phenethyl-9*H*-purin-6-amine (27). Method A; yield 77%: ^{1}H NMR (400 MHz, $CDCl_3$) δ 7.77 (s, 1H), 7.36–7.24 (m, 7H), 6.86 (d, J = 3.96 Hz, 1H), 5.87 (broad s, 1H), 3.86 (s, 3H), 3.03 (t, J = 7.0 Hz, 2H); MS (ESI, M/Z) 394.1, 396.1 $[M + H]^+$; ESI-HRMS calcd for $C_{20}H_{17}N_5{}^{32}S^{35}Cl$ 394.0893, found 394.0890 $[M + H]^+$.

***N*-(Dicyclopropylmethyl)-2-(prop-1-yn-1-yl)-9*H*-purin-6-amine (28).** To a suspension of compound **38** (6 mg, 16.9 μmol) in DMF (1 mL) in glass bomb were added $PdCl_2(PPh_3)_2$ (3.4 mg, 3.38 μmol), copper(I) iodide (0.7 mg, 3.68 μmol) and triethylamine (24 μl, 17 mg, 169 μmol), and propyne gas was condensed in the reaction mixture at −78 °C for 5 min. The reaction mixture was stirred at room temperature for 5 h. After all volatiles were evaporated under reduced pressure, and the residue was purified by silica gel chromatography (dichloromethane : methanol = 20 : 1) to afford compound **28** (2.3 mg, 51%) as a white solid; ^{1}H NMR (400 MHz, CD_3OD) δ 8.07 (s, 1H), 3.70–3.58 (m, 1H), 2.07 (s, 3H), 1.16–1.09 (m, 2H), 0.60–0.54 (m, 2H), 0.48–0.38 (m, 6H); MS (ESI, M/Z) 268.2 $[M + H]^+$; ESI-HRMS calcd for $C_{15}H_{18}N_5$ 268.1562, found 268.1559 $[M + H]^+$.

4-((6-((Dicyclopropylmethyl)amino)-9*H*-purin-2-yl)ethynyl)-benzenesulfonic acid (29). A suspension of compound **38** (9 mg, 25.3 μmol), $PdCl_2(PPh_3)_2$ (3.5 mg, 4.99 μmol), copper(I) iodide (1.2 mg, 6.30 μmol) and triethylamine (35 μl, 25 mg, 251 μmol) in DMF (1 mL) was purged with nitrogen gas for 30 min. To the reaction mixture was added 4-ethynylbenzenesulfonic acid (18 mg, 12.7 mmol), and this mixture was stirred at 50 °C for 15 h. After all volatiles were evaporated under reduced pressure, and the residue was purified by silica gel

chromatography (dichloromethane : methanol : trifluoroacetic acid = 5 : 1 : 0.1) shortly. The crude was purified by HPLC (ACN : 0.1% TFA aqueous solution = 30 : 70 to 20 : 80 in 40 min) to afford compound **29** (5 mg, 48%) as a white solid; Rt = 24.5 min; ^{1}H NMR (400 MHz, CD_3OD) δ 8.39 (s, 1H), 7.92 (d, J = 8.28 Hz, 2H), 7.75 (d, J = 8.36 Hz, 2H), 1.35–1.31 (m, 1H), 1.23–1.19 (m, 2H), 0.68–0.64 (m, 2H), 0.55–0.50 (m, 6H); MS (ESI, M/Z) 408.1, 409.1 $[M - H]^-$; ESI-HRMS calcd for $C_{20}H_{18}N_5O_3{}^{32}S$ 408.1130, found 408.1126 $[M - H]^-$.

6-Chloro-2-iodo-9-(tetrahydro-2*H*-pyran-2-yl)-9*H*-purine (36a). To a mixture of 6-chloro-2-iodopurine (98 mg, 0.35 mmol) and *p*-toluenesulfonic acid (10 mg, 53 μmol) in tetrahydrofuran (6 mL) was added 3,4-dihydro-2*H*-pyran (0.26 mL, 2.8 mmol) at room temperature, and this reaction mixture was refluxed for 16 h. After cooling, the reaction mixture was diluted with ethyl acetate (10 mL) and washed with water (5 mL × 2). The aqueous layer was extracted with ethyl acetate (10 mL × 2), and the combined organic layer was washed with brine, dried ($MgSO_4$), filtered and evaporated under reduced pressure. The crude oil was triturated with hexane to afford compound **36a** (123 mg, 96%) as a yellowish solid; ^{1}H NMR (400 MHz, $CDCl_3$) δ 8.27 (s, 1H), 5.78 (dd, J = 2.4, 10.8 Hz, 1H), 4.20 (d, J = 11.6 Hz, 1H), 3.80 (td, J = 2.8, 11.4 Hz, 1H), 2.18 (d, J = 12.8 Hz, 1H), 2.12–2.09 (m, 1H), 1.99–1.95 (m, 1H), 1.85–1.73 (m, 3H).

6-Chloro-2-iodo-9-methyl-9*H*-purine (36b). To a mixture of 6-chloro-2-iodopurine (61 mg, 0.22 mmol) and potassium carbonate (60 mg, 0.43 mmol) in DMF (3 mL) was added iodomethane (0.5 mL), and this reaction mixture was stirred at room temperature for 1 h. The reaction mixture was diluted with chloroform (10 mL) and washed with water (5 mL × 2). The aqueous layer was extracted with chloroform (10 mL × 2), and the combined organic layer was washed with brine, dried ($MgSO_4$), filtered and evaporated under reduced pressure. The residue was purified by silica gel chromatography (hexane : ethyl acetate = 1 : 1) to afford compound **36b** (44 mg, 70%) as a brown foam; ^{1}H NMR (400 MHz, $CDCl_3$) δ 8.03 (s, 1H), 3.93 (s, 3H).

6-Chloro-2-((5-chlorothiophen-2-yl)ethynyl)-9-(tetrahydro-2*H*-pyran-2-yl)-9*H*-purine (37a). A suspension of compound **36a** (110 mg, 0.30 mmol), $PdCl_2(PPh_3)_2$ (26 mg, 37 μmol), copper(I) iodide (7.3 mg, 38 μmol) and triethylamine (0.26 mL, 189 mg, 1.86 mmol) in 1,4-dioxane (5 mL) was purged with nitrogen gas for 30 min. To the reaction mixture was added 2-chloro-5-ethynylthiophene (106 mg, 0.74 mmol), and this mixture was stirred at room temperature for 1 h. The reaction mixture was diluted with ethyl acetate (15 mL) and washed with water (5 mL × 2). The aqueous layer was extracted with ethyl acetate (10 mL × 2), and the combined organic layer was washed with brine, dried ($MgSO_4$), filtered, and evaporated under reduced pressure. The residue was purified by silica gel chromatography (hexane : ethyl acetate = 3 : 1) to afford compound **37a** (94 mg, 82%) as a brown foam; ^{1}H NMR (400 MHz, $CDCl_3$) δ 8.39 (s, 1H), 7.30 (d, J = 4.0 Hz, 1H), 6.90 (d, J = 4.0 Hz, 1H), 5.85 (dd, J = 2.8 Hz, 10.6 Hz, 1H), 4.23 (d, J = 11.6 Hz, 1H), 3.81 (t, J = 11.6 Hz, 1H), 2.21 (d, J = 10.8 Hz, 1H), 2.13–2.10 (m, 1H), 2.06–1.98 (m, 1H), 1.86–1.76 (m, 3H); MS (ESI, M/Z) 295.0 $[M + H\text{-THP}]^+$; ESI-HRMS calcd for $C_{11}H_5N_4{}^{32}S^{35}Cl_2$ 294.9612, found 294.9611 $[M + H\text{-THP}]^+$.

6-Chloro-2-((5-chlorothiophen-2-yl)ethynyl)-9-methyl-9*H*-purine (37b). Compound **36b** (9.5 mg, 32.3 μmol) was converted to compound **37b** (10.0 mg, 99%) as a white solid, using similar procedure used in the preparation of compound **37a**; purified by silica gel column chromatography (dichloromethane : ethyl acetate = 2 : 1); ^{1}H NMR (400 MHz, $CDCl_3$) δ 8.16 (s, 1H), 7.30 (d, J = 4.0 Hz, 1H), 6.89 (d, J = 4.0 Hz, 1H), 3.97 (s, 3H); MS (ESI, M/Z) 308.9 $[M + H\text{-THP}]^+$; ESI-HRMS calcd for $C_{12}H_7N_4{}^{32}S^{35}Cl_2$ 308.9768, found 308.9773 $[M + H]^+$.

6-Chloro-2-((5-chlorothiophen-2-yl)ethynyl)-9*H*-purine (37c). A mixture of compound **37a** (93 mg, 0.32 mmol) in trifluoroacetic acid and dichloromethane (1 : 9, 6 mL) solution was stirred at room temperature for 2 h. After all volatiles were evaporated under reduced pressure, the crude was purified by silica gel column chromatography (dichloromethane : methanol = 50 : 1) to afford compound **37c** (64 mg, 88%) as a white solid; ^{1}H NMR (400 MHz, $CDCl_3$) δ 8.61 (s, 1H), 7.39 (d, J = 4.0 Hz, 1H), 7.06 (d, J = 4.0 Hz, 1H); MS (ESI, M/Z) 294.9.0, 296.9, 299.0 $[M + H]^+$; ESI-HRMS calcd for $C_{11}H_5N_4{}^{32}S^{35}Cl_2$ 294.9612, found 294.9611 $[M + H]^+$.

***N*-(Dicyclopropylmethyl)-2-iodo-9*H*-purin-6-amine (38).** To a solution of 6-chloro-2-iodopurine (30 mg, 0.107 mmol) and *N*,*N*-dicyclopropylmethylamine hydrochloride (79 mg, 0.535 mmol) in isopropanol (2 mL) was added diisopropylethylamine (0.2 mL, 138 mg, 1.07 mmol) at room temperature, and the reaction mixture was heated at 90 °C in a microwave synthesizer for 3 h. The reaction mixture was diluted with ethyl acetate (10 mL) and washed with water (5 mL × 2). After all volatiles were evaporated under reduced pressure, the crude was purified by silica gel column chromatography (dichloromethane : methanol = 50 : 1) to afford compound **38** (37 mg, 97%) as a white solid; ^{1}H NMR (400 MHz, $CDCl_3$) δ 8.09 (s, 1H), 3.50 (s, 1H), 0.62–0.42 (m, 10H); MS (ESI, M/Z) 356.0 $[M + H]^+$; ESI-HRMS calcd for $C_{12}H_{15}IN_5$ 356.0372 found 356.0378 $[M + H]^+$.

***N*-Cyclopentyl-2-iodo-9*H*-purin-6-amine (39).** To a solution of 6-chloro-2-iodopurine (24 mg, 86 μmol) and cyclopentylamine (12 μL, 11 mg, 0.128 mmol) in ethanol was added triethylamine (13 mg, 18 μL, 0.128 mmol) at room temperature, and the reaction mixture was refluxed for 15 h. After all volatiles were evaporated under reduced pressure, the crude was purified by silica gel column chromatography (dichloromethane : methanol = 50 : 1) to afford compound **39** (14 mg, 48%) as a white solid; ^{1}H NMR (400 MHz, $CDCl_3$) δ 7.92 (s, 1H), 4.61 (broad s, 0.25H; NH), 2.20–2.15 (m, 2H), 1.81–1.74 (m, 5H), 1.62–1.59 (m, 2H); MS (ESI, M/Z) 294.9.0, 296.9, 299.0 $[M + H]^+$; ESI-HRMS calcd for $C_{11}H_5N_4{}^{32}S^{35}Cl_2$ 294.9612, found 294.9611 $[M + H]^+$.

Conclusions

We have identified novel hA_3AR antagonists based on an adenine scaffold. N^6-Alkyl, cycloalkyl and arylalkyl substitutions

combined with an A_3AR-favoring 2-((5-chlorothiophen-2-yl)ethynyl) group tended to favor A_3AR. N^6-Propyladenine derivative **17** displayed the highest hA_3AR selectivity (~1000-fold). N^6-Phenylethyl analogue **24** was 135-fold hA_3AR-selective with a K_i of 13 nM. Thus, in attempting to map the SAR of AR nucleoside agonists onto the adenine scaffold, the affinity at A_3AR predominates in this series, even with A_1AR-favoring groups. Compounds initially predicted to combine A_1/$_3$AR selectivity did not bind appreciably at the A_1AR. Although we achieved selectivity at hA_3AR, but not rodent A_3AR, the SAR of nucleoside AR agonists was mostly not recapitulated in adenine AR antagonists. We have used molecular modeling and docking to characterize the recognition of a selective adenine derivative **17** at its target hA_3AR to probe its overlay with similarly derivatized A_3AR agonist **10**. Modeling suggested an alternative, inverted binding mode with the key N250$^{6.55}$ H-bonding to the adenine N^3 and N^9, instead of N^6 and N^7 as in adenosine agonists. These adenine derivatives may be useful as pharmacological probes of the hA_3AR. Thus, we have discovered potent and selective A_3AR antagonists, potentially useful in inflammatory conditions and glaucoma, with an understanding of their receptor interactions.

Abbreviations

AN	Acetonitrile
AR	Adenosine receptor
BM	Binding mode
CHO	Chinese hamster ovary
DCM	Dichloromethane
DHP	Dihydropyran
DIPEA	Diisopropylethylamine
DMF	*N*,*N*-Dimethylformamide
EL	Extracellular loop
GPCR	G protein-coupled receptor
HEK	Human embryonic kidney
IE	Interaction energy
MD	Molecular dynamics
MRS1754	8-[4-[[(4-Cyano)phenylcarbamoylmethyl]oxy] phenyl]-1,3-di-(*n*-propyl)xanthine
NECA	5′-*N*-Ethylcarboxamidoadenosine
RMSD	Root mean squared deviation
TBAP	Tetrabutylammonium dihydrogen phosphate
THP	Tetrahydropyran
TM	Transmembrane helical domain

Conflicts of interest

There are no conflicts of interest to declare.

Acknowledgements

We thank the NIH Intramural Research Program (NIDDK, ZIADK31117), National Cancer Institute (R01CA169519) and National Heart Lung Institute (R01HL077707) for support and John Lloyd (NIDDK) for mass spectral determinations.

Notes and references

1 C. E. Müller and K. A. Jacobson, *Biochim. Biophys. Acta, Biomembr.*, 2011, **1808**, 1290–1308.
2 W. Jespers, A. C. Schiedel, L. H. Heitman, R. M. Cooke, L. Kleene, G. J. P. Van Westen, D. E. Gloriam, C. E. Müller, E. Sotelo and H. Gutiérrez-de-Terán, *Trends Pharm. Sci.*, 2018, **39**, 75–89.
3 V. P. Jaakola, M. T. Griffith, M. A. Hanson, V. Cherezov, E. Y. T. Chien, J. R. Lane, A. P. IJzerman and R. C. Stevens, *Science*, 2008, **322**, 1211–1217.
4 F. Xu, H. Wu, V. Katritch, G. W. Han, K. A. Jacobson, Z.-G. Gao, V. Cherezov and R. C. Stevens, *Science*, 2011, **332**(6027), 322–327.
5 K. A. Jacobson, Z. G. Gao, S. Paoletta, E. Kiselev, S. Charkaborty, P. S. Jayasekara, R. Balasubramanian and D. K. Tosh, *Comput. Struct. Biotechnol. J.*, 2015, **13**, 286–298.
6 A. Glukhova, D. M. Thal, A. T. Nguyen, E. A. Vecchio, M. Jörg, P. J. Scammells, L. T. May, P. M. Sexton and A. Christopoulos, *Cell*, 2017, **168**, 867–877.
7 R. K. Y. Cheng, E. Segala, N. Robertson, F. Deflorian, A. S. Doré, J. C. Errey, C. Fiez-Vandal, F. H. Marshall and R. M. Cooke, *Structure*, 2017, **25**, 1275–1285.
8 B. Sun, P. Bachhawat, M. Ling-Hon Chu, M. Wood, T. Ceska, Z. A. Sands, J. Mercier, F. Lebon, T. S. Kobilka and B. K. Kobilka, *Proc. Natl. Acad. Sci. U. S. A.*, 2017, **114**, 2066–2071.
9 P. Rucktooa, R. K. Y. Cheng, E. Segala, T. Geng, J. C. Errey, G. A. Brown, R. Cooke, F. H. Marshall and A. S. Doré, *Sci. Rep.*, 2018, **8**, 41, DOI: 10.1038/s41598-017-18570-w.
10 D. Ukena, W. L. Padgett, O. Hong, J. W. Daly and R. A. Olsson, *FEBS Lett.*, 1987, **215**, 203–208.
11 H. Harada, O. Asano, Y. Hoshino, S. Yoshikawa, M. Matsukura, Y. Kabasawa, J. Niijima, Y. Kotake, N. Watanabe, T. Kawata, T. Inoue, T. Horizoe, N. Yasuda, H. Minami, K. Nagata, M. Murakami, J. Nagaoka, S. Kobayashi, I. Tanaka and S. Abe, *J. Med. Chem.*, 2001, **44**, 170–179.
12 A. Thomas, M. Buccioni, D. Dal Ben, C. Lambertucci, G. Marucci, C. Santinelli, A. Spinaci, S. Kachler, K.-N. Klotz and R. Volpini, *ChemMedChem*, 2016, **11**, 1829–1939.
13 P. L. Martin, R. J. Wysocki, R. J. Barrett, J. M. May and J. Linden, *J. Pharmacol. Exp. Ther.*, 1996, **276**, 490–499.
14 M. Perreira, J. K. Jiang, A. Klutz, Z. G. Gao, A. Shainberg, C. Lu, C. J. Thomas and K. A. Jacobson, *J. Med. Chem.*, 2005, **48**, 4910–4918.
15 B. K. Trivedi, A. J. Bridges, W. C. Patt, S. R. Priebe and R. F. Bruns, *J. Med. Chem.*, 1989, **32**, 8–11.
16 P. Franchetti, L. Cappellacci, P. Vita, R. Petrelli, A. Lavecchia, S. Kachler, K.-N. Klotz, I. Marabese, L. Luongo, S. Maione and M. Grifantini, *J. Med. Chem.*, 2009, **52**, 2393–2406.
17 Z. G. Gao, J. B. Blaustein, A. S. Gross, N. Melman and K. A. Jacobson, *Biochem. Pharmacol.*, 2003, **65**, 1675–1684.
18 D. K. Tosh, S. Paoletta, F. Deflorian, K. Phan, S. M. Moss, Z. G. Gao, X. Jiang and K. A. Jacobson, *J. Med. Chem.*, 2012, **55**, 8075–8090.
19 E. Camaioni, S. Costanzi, S. Vittori, R. Volpini, K. N. Klotz and G. Cristalli, *Bioorg. Med. Chem.*, 1998, **6**, 523–533.

20 D. Dal Ben, M. Buccioni, C. Lambertucci, A. Thomas, K.-N. Klotz, S. Federico, B. Cacciari, G. Spalluto and R. Volpini, *Eur. J. Med. Chem.*, 2013, **70**, 525–535.
21 C. Lambertucci, I. Antonini, M. Buccioni, D. Dal Ben, D. D. Kachare, R. Volpini, K.-N. Klotz and G. Cristalli, *Bioorg. Med. Chem.*, 2009, **17**, 2812–2822.
22 K. Endo, K. Deguchi, H. Matsunaga, K. Tomaya and K. Yamada, *Bioorg. Med. Chem.*, 2014, **22**, 3072–3082.
23 M. Peleli and M. Carlström, *Mol. Aspects Med.*, 2017, **55**, 62–74.
24 L. T. May, S. J. Briddon and S. J. Hill, *Mol. Pharmacol.*, 2010, **77**, 678–686.
25 S. J. Hill, L. T. May, B. Kellam and J. Woolard, *Br. J. Pharmacol.*, 2014, **171**, 1102–1113.
26 A. Knight, J. L. Hemmings, I. Winfield, M. Leuenberger, E. Frattini, B. G. Frenguelli, S. J. Dowell, M. Lochner and G. Ladds, *J. Med. Chem.*, 2016, **59**, 947–964.
27 D. Dal Ben, M. Buccioni, C. Lambertucci, S. Kachler, N. Falgner, G. Marucci, A. Thomas, G. Cristalli, R. Volpini and K. N. Klotz, *Biochem. Pharmacol.*, 2014, **87**, 321–331.
28 D. K. Tosh, F. Deflorian, K. Phan, Z. G. Gao, T. Wan, E. Gizewski, J. A. Auchampach and K. A. Jacobson, *J. Med. Chem.*, 2012, **55**, 4847–4860.
29 S. Paoletta, D. K. Tosh, A. Finley, E. Gizewski, S. M. Moss, Z. G. Gao, J. A. Auchampach, D. Salvemini and K. A. Jacobson, *J. Med. Chem.*, 2013, **56**, 5949–5963.
30 D. K. Tosh, A. Finley, S. Paoletta, S. M. Moss, Z. G. Gao, E. Gizewski, J. A. Auchampach, D. Salvemini and K. A. Jacobson, *J. Med. Chem.*, 2014, **57**, 9901–9914.
31 K. A. Jacobson, Z. G. Gao, S. Tchilibon, H. T. Duong, B. V. Joshi, D. Sonin and B. T. Liang, *J. Med. Chem.*, 2005, **48**, 8103–8107.
32 W. H. Moos, D. S. Szotek and R. F. Bruns, *J. Med. Chem.*, 1985, **28**, 1383–1384.
33 E. Elzein and J. Zablocki, *Expert Opin. Invest. Drugs*, 2008, **17**, 1901–1910.
34 Y. C. Cheng and W. H. Prusoff, *Biochem. Pharmacol.*, 1973, **22**, 3099–3108.
35 D. K. Tosh, S. Crane, Z. Chen, S. Paoletta, Z. G. Gao, E. Gizewski, J. A. Auchampach, D. Salvemini and K. A. Jacobson, *ACS Med. Chem. Lett.*, 2015, **6**, 804–808.
36 D. E. Pires, T. L. Blundell and D. B. Ascher, *J. Med. Chem.*, 2015, **58**, 4066–4072.
37 P. Matricon, A. Ranganathan, E. Warnick, Z. G. Gao, C. Lambertucci, G. Marucci, A. Ezzati, A. Rudling, M. Jaiteh, D. Dal Ben, K. A. Jacobson and J. Carlsson, *Sci. Rep.*, 2017, **7**(1), 6398, DOI: 10.1038/s41598-017-04905-0.
38 K. A. Jacobson, S. Merighi, K. Varani, P. A. Borea, S. Baraldi, M. A. Tabrizi, R. Romagnoli, P. G. Baraldi, A. Ciancetta, D. K. Tosh, Z. G. Gao and S. Gessi, *Med. Res. Rev.*, 2017, **38**, 1031–1072.
39 D. Dorotea, A. Cho, G. Lee, G. Kwon, J. Lee, P. K. Sahu, L. S. Jeong, D. R. Cha and H. Ha, *Exp. Mol. Med.*, 2018, **50**, 38, DOI: 10.1038/s12276-018-0053-x.
40 X.-d. Ji, Y. C. Kim, D. G. Ahern, J. Linden and K. A. Jacobson, *Biochem. Pharmacol.*, 2001, **61**, 657–663.
41 X. Hou, M. S. Majik, K. Kim, Y. Pyee, Y. Lee, V. Alexander, H. J. Chung, H. W. Lee, G. Chandra, J. H. Lee, S. G. Park, W. J. Choi, H. O. Kim, K. Phan, Z. G. Gao, K. A. Jacobson, S. Choi, S. K. Lee and L. S. Jeong, *J. Med. Chem.*, 2012, **55**, 342–356.
42 J. Besnard, G. F. Ruda, V. Setola, K. Abecassis, R. M. Rodriguiz, X. P. Huang, S. Norval, M. F. Sassano, A. I. Shin, L. A. Webster, F. R. Simeons, L. Stojanovski, A. Prat, N. G. Seidah, D. B. Constam, G. R. Bickerton, K. D. Read, W. C. Wetsel, I. H. Gilbert, B. L. Roth and A. L. Hopkins, *Nature*, 2012, **492**, 215–220.
43 J. A. Ballesteros and H. Weinstein, *Methods Neurosci.*, 1995, **25**, 366–428.
44 D. K. Tosh, K. Phan, F. Deflorian, Q. Wei, Z. G. Gao and K. A. Jacobson, *ACS Med. Chem. Lett.*, 2011, **2**, 626–631.

